Applied Ocean Research 68 (2017) 249–261

Contents lists available at ScienceDirect

Applied Ocean Research

journal homepage: www.elsevier.com/locate/apor

Identification-based simplified model of large container ships using support vector machines and artificial bee colony algorithm

Man Zhu[a,*], Axel Hahn[a], Yuan-Qiao Wen[b,c], Andre Bolles[d]

[a] Computer Science, Carl-von-Ossietzky University of Oldenburg, 26121 Oldenburg, Germany
[b] School of Navigation, Wuhan University of Technology, 430063 Hubei, China
[c] Hubei Key Laboratory of Inland Shipping Technology, 430063 Hubei, China
[d] Institute for Information Technology, 26121 Oldenburg, Germany

ARTICLE INFO

Article history:
Received 31 October 2016
Received in revised form 24 August 2017
Accepted 7 September 2017
Available online 23 September 2017

Keywords:
Nonlinear ship dynamics
Simplified ship models
Large ships
Support vector machines
Artificial bee colony algorithm
Parameter identification

ABSTRACT

The 6 degrees of freedom (DOF) model with a high degree of complexity for capturing ship dynamics is generally able to track the nonlinear and coupling dynamics of ships. However, the 6 DOF model makes challenges in estimating model coefficients and designing the model-based control. Therefore, simplified ship dynamic models within allowed accuracy are essential. This paper simplified the 6 DOF nonlinear dynamic model of ships into two decoupled models including the speed model and the steering model through reasonable assumptions. Those models were tested through maneuvering simulations of a container ship with a 4 DOF dynamic model. Support vector machines (SVM) optimized by the artificial bee colony algorithm (ABC) was used to identify parameters of speed and steering models by analyzing the rudder angle, propeller shaft speed, surge and sway velocities, and yaw rate from simulated data extracted from a series of maneuvers made by the container ship. Comparisons with the first order linear and nonlinear Nomoto models show that the simplified nonlinear steering model can capture more complicated dynamics and performs better. Additionally, comparisons among three different parameter identification methods demonstrate similar identification results but the different performance involving the applicability and effectiveness. SVM optimized by ABC is relatively convenient and effective for parameter identification of ship simplified dynamic models.

1. Introduction

With the development of advanced control techniques such as the linear quadratic Gaussian control (LQG), the state feedback linearization, the integrator backstepping, and the sliding-mode control [1], model-based control has become the state-of-the-art for steering and positioning ships to enhance performance of ships. Due to the high cost and risk of using full-size ships to test advanced control methodologies, a scaled-model ship is always applied to evaluate ship control approaches [2]. These studies, to some degree, can facilitate the effectiveness of their control techniques, but the scale effect caused by differences between scaled-model ships and large ships makes the application of these control techniques to large ships a challenging task. A large container ship [3] is used to remedy this situation in this paper. The dynamics of this container ship in 4 degrees of freedom (4 DOF), i.e., translational motions of surge and sway, and rotational motions of roll and yaw, are described in reality by a set of complex differential equations which will be presented in the next section. These sufficiently accurate equations satisfy simulation study purposes about assessing maneuverability of ships. With respect to the ship control, however, they will exponentially increase complexity of the control designs, and make the reasonable estimation of parameters of the ship dynamic model a tough task. An adequate ship dynamic model with reasonable parameters is imperative for the studies of control designs and simulations.

Therefore, aiming at determining a desirable ship dynamic model with relatively acceptable complexity for control designs, this paper addresses the simplifications of the nonlinear and coupling dynamic model for a large container ship by only considering the decoupled speed and steering motions. Recently, studies have been reported on applying the simplified ship dynamic model to ship control designs. For instance, Zwierzewicz [4] linearized the nonlinear ship model of Norrbin type, and then applied it to adaptive control approaches to test the ship course-keeping control system. Besides, Sonnenburg [5] used a backstepping trajectory

* Corresponding author.
E-mail address: man.zhu@uni-oldenburg.de (M. Zhu).

http://dx.doi.org/10.1016/j.apor.2017.09.006
0141-1187/

controller to track the Ribcraft USV's trajectories generated by the first order linear Nomoto model with the linear sideslip model and simplified speed model, and the references therein. Obviously, the authors are mainly using scaled-model ships for their work, which in turn illustrates that the goal of this paper about simplifying the complex model of large ships is meaningful.

After selecting the suitable ship dynamic model for control designs, parameter identification of the ship dynamic model is another task of much importance. The main methods for estimating the maneuvering model include towing-tank experiments, captive model experiments [6], computational fluid dynamics (CFD) and system identification combined with full-scale or free-running model [7]. Among these methods, system identification combined with full-scale or free-running model is becoming an attractive and sufficient technique for estimating ship maneuvering model due to its relatively high cost-effectiveness.

System identification is a very large topic with different techniques that depend on the characters of models to be estimated: linear, nonlinear, hybrid, nonparametric, etc. [8]. Various conventional system identification methods such as the least squares method (LS) [7], the maximum likelihood method (ML) [9] and the extended Kalman filter (EKF) [10] have been successfully applied to estimate the ship maneuvering model. During recent years, a variety of new methods based on the modern artificial intelligent technology, such as the artificial neural network (ANN) [11], the genetic algorithm (GA) [12] and the support vector machines (SVM) [13,14] have been successfully used to system identification of the ship maneuvering model. Comparatively, SVM directs at finite samples, which requires no initial identification of parameters but has good generalization performance and global optimum. Note that the coefficients of variables in the regression model are sensitive to the structural parameters in SVM, such as the insensitivity factor, the regularization parameter, and kernel parameters. Using trails is a general way to determine parameters in SVM. In contrast, it seems a cost-effective way to optimize parameters in SVM by intelligent algorithms instead of using trails. Taking the research [15] as an example, the particle swarm optimization algorithm (PSO) is incorporated into SVM to obtain the optimized structural factors in SVM, and the SVM regression results agree well with the experimental results. Inspired by this research, and the better performance of ABC than PSO [16,17], this paper is the first proposing SVM optimized by ABC to identify the simplified dynamic model of large ships by using simulated data.

The main contributions of this paper are summarized as follows: First, the nonlinear and coupling dynamic model of ships is simplified into a 3 DOF nonlinear dynamic model including decoupled speed and steering models. This model can be easily modified to either a 3 DOF model for the large ship trajectory tracking, and path following, etc., or a steering model for large ship autopilot control designs. Furthermore, to date, SVM optimized by ABC is the first time to be used for parameter identification of the simplified dynamic model of large container ships. This boosts the application of SVM in marine research field while declaring the solution of optimizing structural parameters in SVM. To the best knowledge of authors, the application of SVM optimized by ABC to parameter identification of the ship dynamic model has not been considered in open literatures.

This paper is organized as follows. Section 2 describes an overview of the nonlinear model of a container ship, and addresses the simplification of the complex model. In Section 3, the formulations of SVM and ABC, and construction of samples for identification are presented, respectively. The simulated maneuvers of the large container ship are used in Section 4 as training samples and validation samples for parameter identification of the simplified ship dynamic model, and comparisons among three steering models, and three parameter identification methods are carried out, respectively. Finally, concluding remarks are summarized in Section 5.

Table 1
Notation from SNAME.

DOF	Motions	Forces	Linear velocity	Positions
1	Surge	X	u	x
2	Sway	Y	v	y
3	Heave	Z	w	z
	Rotations	Moments	Angular velocity	Rotation angles
4	Roll	K	p	φ
5	Pitch	M	q	θ
6	Yaw	N	r	ψ

2. Dynamic model of ships

For ships moving in 6 DOF, six independent coordinates are necessary to determine the position and orientation. The first three coordinates and their time derivatives correspond to the position and translational motion along the x, y and z, while the last three coordinates and their time derivatives are used to describe the orientation and rotational motion [1]. Generally, the two reference frames shown in Fig. 1 consisted of a body-fixed frame and an earth-fixed frame are used to describe 6 DOF dynamics which can be analyzed through the Newton–Euler formulation. The nonlinear 6 DOF dynamic model of a ship can be expressed in the body-fixed frame as [3]

$$\dot{\boldsymbol{\eta}} = \mathbf{J}(\boldsymbol{\eta})\boldsymbol{\upsilon}, \tag{1}$$

$$\boldsymbol{M}\dot{\boldsymbol{\upsilon}} + \boldsymbol{C}(\boldsymbol{\upsilon})\boldsymbol{\upsilon} + \mathbf{D}(\boldsymbol{\upsilon})\boldsymbol{\upsilon} + \mathbf{g}(\boldsymbol{\eta}) = \boldsymbol{\tau}_{ext} + \boldsymbol{\tau}, \tag{2}$$

where $\boldsymbol{\upsilon} = [u, v, w, p, q, r]^T$ is the spatial velocity state vector, $\boldsymbol{\eta} = \left[x, y, z, \varphi, \theta, \psi\right]^T$ presents the position and orientation states, $\boldsymbol{J}(\boldsymbol{\eta}) = f(\varphi, \theta, \psi)$ is the transformation matrices between variants in the body-fixed frame and earth-fixed frame, $\boldsymbol{M}$ is the mass matrix, $\boldsymbol{C}(\boldsymbol{\upsilon})$ is the Coriolis and centripetal matrix, $\boldsymbol{D}(\boldsymbol{\upsilon})$ is the damping matrix, $\mathbf{g}(\boldsymbol{\eta})$ manifests the effects of buoyancy's interaction with gravity, $\boldsymbol{\tau} = [X, Y, Z, K, a, N]^T$ denotes the actuator forces and moments generated by a set of propellers with revolutions per second $\mathbf{n} = [n_1, n_2, \ldots, n_{p1}]^T$ and a set of control surfaces with angles $\boldsymbol{\delta} = [\delta_1, \delta_2, \ldots, \delta_{p2}]^T$, $\boldsymbol{\tau}_{ext}$ is the external disturbances from currents, wave, etc. The notation from SNAME used in this paper are presented in Table 1.

2.1. Nonlinear model of a large container ship

The study of the maneuverability of surface ships are mainly considered for studying the horizontal motions of ships such as surge, sway and yaw with more importance given to the last two highly coupled motions, known as the steering model. However, for the high speed container ship, the roll effects cannot be ignored. Hence, the nonlinear roll-coupled steering model for the high speed container ship is written as [18]

$$(m - X_{\dot{u}})\dot{u} - (m - Y_{\dot{v}})vr = X, \tag{3}$$

$$(m - Y_{\dot{v}})\dot{v} + (m - X_{\dot{u}})ur - Y_{\dot{r}}\dot{r} = Y, \tag{4}$$

$$(I_x - K_{\dot{p}})\dot{p} = K - WG\bar{M}_T\varphi, \tag{5}$$

$$(I_z - N_{\dot{r}})\dot{r} + N_{\dot{v}}\dot{v} = N, \tag{6}$$

where

$$X = X(u) + (1 - t)T + X_{vr}vr + X_{vv}v^2 + X_{rr}r^2 + X_{\varphi\varphi}\varphi^2 + X_\delta \sin\delta + X_{ext}, \tag{7}$$

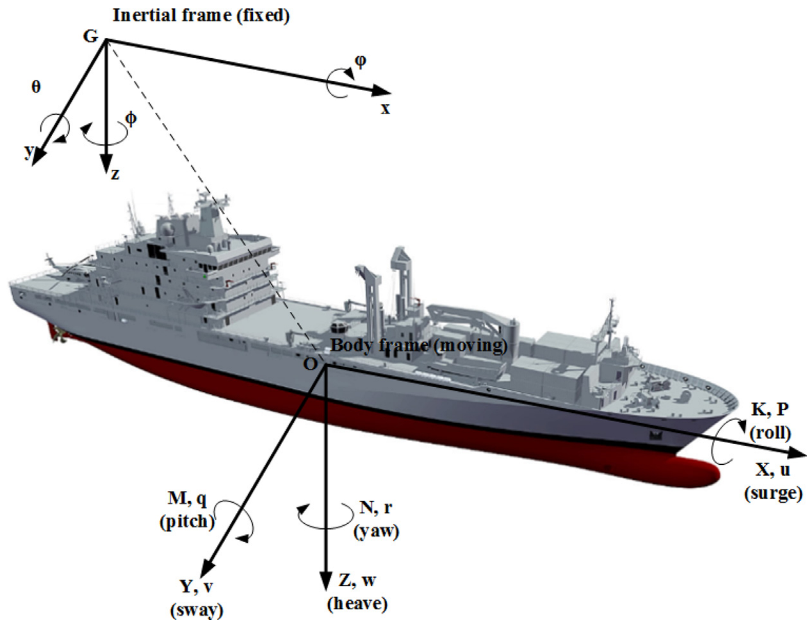

Fig. 1. Reference frames for ships.

$$Y = Y_v v + Y_r r + Y_\varphi \varphi + Y_p p + Y_{vvv} v^3 + Y_{rrr} r^3 + Y_{vvr} v^2 r + Y_{vrr} v r^2 + Y_{vv\varphi} v^2 \varphi + Y_{v\varphi\varphi} v \varphi^2 + Y_{rr\varphi} r^2 \varphi + Y_{r\varphi\varphi} r \varphi^2 + Y_\delta \cos\delta + Y_{ext}, \tag{8}$$

$$K = K_v v + K_r r + K_\varphi \varphi + K_p p + K_{vvv} v^3 + K_{rrr} r^3 + K_{vvr} v^2 r + K_{v\varphi\varphi} v \varphi^2 + K_{vrr} v r^2 + K_{vv\varphi} v^2 \varphi + K_{rr\varphi} r^2 \varphi + K_{r\varphi\varphi} r \varphi^2 + K_\delta \cos\delta + K_{ext}, \tag{9}$$

$$N = N_v v + N_r r + N_\varphi \varphi + N_p p + N_{vvv} v^3 + N_{rrr} r^3 + N_{vvr} v^2 r + N_{vrr} v r^2 + N_{vv\varphi} v^2 \varphi + N_{v\varphi\varphi} v \varphi^2 + N_{rr\varphi} r^2 \varphi + N_{r\varphi\varphi} r \varphi^2 + N_\delta \cos\delta + N_{ext}. \tag{10}$$

The variants are used in accordance with SNAME shown in Table 1. $\dot{u}$ and $\dot{v}$ are linear accelerations in the x and y direction, respectively, $\dot{p}$ and $\dot{r}$ are angular accelerations in the x and z direction, respectively, I_x and I_z are the inertial moments about the x and z axis, respectively, m is the mass of the ship, W is the weight of water displaced by the ship's hull, $G\bar{M}_T$ is the transverse metacentric height, $X(u)$ is the velocity dependent damping function, t is the thrust deduction factor, T is the propeller thrust and δ is the rudder angle, X_{ext}, Y_{ext}, K_{ext} and N_{ext} are forces or moments due to external disturbances. The left nomenclatures are hydrodynamic derivatives and the details referred to [11]. The principal particulars of the container ship are given in Table 2.

2.2. Simplified ship dynamic model

In order to decrease the complexity of ship controller designs, the complex 6 DOF model of ships can be simplified through a set of reasonable assumptions as follows: (1) surface ships are moving in a horizontal plane in the ideal fluid; (2) ships masses are uniformly distributed; (3) the body-fixed frame coincides with the center of gravity; (4) both the center of gravity and the center of buoyancy point vertically along the z axis; (5) ships are the port-starboard symmetry and (6) the horizontal dynamic motions are decomposed into speed (surge) and steering (sway and yaw) motions [19].

Table 2
Principal particulars of the container ship.

Particulars	Values
Length between perpendiculars	175 m
Length over all	178 m
Breadth	25.4 m
Draft at the fore end	8 m
Draft at the aft end	9 m
Mean draft	8.5 m
Displacement volume	21,222 m^3
Height from keel to transverse metacenter	10.39 m
Height from keel to center of buoyancy	4.6145 m
Block coefficient	0.559
Rudder area	33.0376 m^2
Aspect ratio	1.8219
Propeller diameter	6.533 m

Therefore, the two mainly concerned models are steering and speed models. The former model is used to control the yaw angle by using the rudder angle as the control variable. The latter model is applied to control the ship speed by varying the propeller shaft speed. To clearly explain the simplified dynamic models, the 3 DOF dynamic model governed based on above assumptions can be introduced as [3]

$$\boldsymbol{M}\dot{\boldsymbol{v}} + \boldsymbol{C}(\boldsymbol{v})\boldsymbol{v} + \boldsymbol{D}(\boldsymbol{v})\boldsymbol{v} + \boldsymbol{g}(\boldsymbol{\eta}) = \boldsymbol{\tau}, \tag{11}$$

where the expression of every symbol is shown as

$$\mathbf{M} = \mathbf{M_{RB}} + \mathbf{M_A} = \begin{bmatrix} m & 0 & 0 \\ 0 & m & mx_g \\ 0 & mx_g & I_z \end{bmatrix} + \begin{bmatrix} -X_{\dot{u}} & 0 & 0 \\ 0 & -Y_{\dot{v}} & -Y_{\dot{r}} \\ 0 & -N_{\dot{v}} & -N_{\dot{r}} \end{bmatrix} = \begin{bmatrix} m - X_{\dot{u}} & 0 & 0 \\ 0 & m - Y_{\dot{v}} & mx_g - Y_{\dot{r}} \\ 0 & mx_g - N_{\dot{v}} & I_z - N_{\dot{r}} \end{bmatrix}, \tag{12}$$

$$
\begin{aligned}
\boldsymbol{C}(\boldsymbol{\upsilon}) &= \mathbf{C}_{\boldsymbol{RB}}(\boldsymbol{\upsilon}) + \mathbf{C}_{\mathbf{A}}(\boldsymbol{\upsilon}) = \begin{bmatrix} 0 & 0 & -m(x_g r + v) \\ 0 & 0 & mu \\ m(x_g r + v) & -mu & 0 \end{bmatrix} \\
&+ \begin{bmatrix} 0 & 0 & Y_{\dot v} v + \frac{1}{2}(Y_{\dot r} + N_{\dot v}) r \\ 0 & 0 & -X_{\dot u} u \\ -Y_{\dot v} v - \frac{1}{2}(Y_{\dot r} + N_{\dot v}) r & X_{\dot u} u & 0 \end{bmatrix} \\
&= \begin{bmatrix} 0 & 0 & (Y_{\dot v} - m)v + \left(\frac{1}{2}Y_{\dot r} + \frac{1}{2}N_{\dot v} - m x_g\right) r \\ 0 & 0 & (m - X_{\dot u})u \\ -(Y_{\dot v} - m)v - \left(\frac{1}{2}Y_{\dot r} + \frac{1}{2}N_{\dot v} - m x_g\right) r & -(m - X_{\dot u})u & 0 \end{bmatrix},
\end{aligned}
\tag{13}
$$

$$
\begin{aligned}
\mathbf{D}(\boldsymbol{\upsilon}) &= \mathbf{D}_L + \mathbf{D}_{NL}(\boldsymbol{\upsilon}) = \begin{bmatrix} -X_u & 0 & 0 \\ 0 & -Y_v & -Y_r \\ 0 & -N_v & -N_r \end{bmatrix} \\
&+ \begin{bmatrix} -X_{|u|u}|u| & 0 & 0 \\ 0 & -Y_{|v|v}|v| - Y_{|r|v}|r| & -Y_{|v|r}|v| - Y_{|r|r}|r| \\ 0 & -N_{|v|v}|v| - N_{|r|v}|r| & -N_{|v|r}|v| - N_{|r|r}|r| \end{bmatrix} \\
&= \begin{bmatrix} -X_u - X_{|u|u}|u| & 0 & 0 \\ 0 & -Y_v - Y_{|v|v}|v| - Y_{|r|v}|r| & -Y_r - Y_{|v|r}|v| - Y_{|r|r}|r| \\ 0 & -N_v - N_{|v|v}|v| - N_{|r|v}|r| & -N_r - N_{|v|r}|v| - N_{|r|r}|r| \end{bmatrix},
\end{aligned}
\tag{14}
$$

$$\mathbf{g}(\boldsymbol{\eta}) = [0 \;\; 0 \;\; 0]^T, \tag{15}$$

$$\boldsymbol{\tau} = [T_{|n|n}|n|n \qquad Y_\delta \delta \qquad N_\delta \delta]^T, \tag{16}$$

with n presenting the propeller shaft speed and $T_{|n|n}$ coefficient depending on the diameter of the propeller and the density of the water.

Note that the external disturbances are important for testing the performance and robustness of ship controllers but negatively affect the parameter identification of the ship dynamic model. They are not presented in the above equations and also ignored in the process of making ship maneuvering simulation to fulfill the goal of our study about evaluating the performance of parameter identification methods which does not prefer data corrupted by noises. Mathematical models describing external disturbances such as wave- and wind-induced forces and moments refer to chapter 8 about environmental forces and moments in [1].

2.2.1. Speed model

Given that the turn rate (r) and sway velocity (v) are small enough, and their effects on the surge motion are ignored, the speed dynamic model can be simplified to

$$(m - X_{\dot u})\dot u = X_u u + X_{|u|u}|u|u + X_{uuu}u^3 + T_{|n|n}|n|n, \tag{17}$$

which is the second order modulus model with an extra third order term in surge. The reason for adding the third order term is that it shows the best fit to the experimental data [20]. For the control purpose, it is not necessary to compute all hydrodynamic derivatives which define ship characteristics and its complete behaviors. Hence, Eq. (17) can be reorganized as

$$\dot u = \frac{X_u}{m - X_{\dot u}} u + \frac{X_{|u|u}}{m - X_{\dot u}}|u|u + \frac{X_{uuu}}{m - X_{\dot u}} u^3 + \frac{T_{|n|n}}{m - X_{\dot u}}|n|n. \tag{18}$$

2.2.2. Steering model

The remaining steering model describing sway and yaw motions is obtained from Eq. (11) based on the constant surge speed (u_0)

$$
\begin{aligned}
&\begin{bmatrix} m - Y_{\dot v} & m x_g - Y_{\dot r} \\ m x_g - N_{\dot v} & I_z - N_{\dot r} \end{bmatrix} \begin{bmatrix} \dot v \\ \dot r \end{bmatrix} \\
&= \begin{bmatrix} -Y_v - Y_{|v|v}|v| - Y_{|r|v}|r| & (m - X_{\dot u})u_0 - Y_r - Y_{|v|r}|v| - Y_{|r|r}|r| \\ -(m - X_{\dot u})u_0 - N_v - N_{|v|v}|v| - N_{|r|v}|r| & -N_r - N_{|v|r}|v| - N_{|r|r}|r| \end{bmatrix} \begin{bmatrix} v \\ r \end{bmatrix} \\
&+ \begin{bmatrix} Y_\delta \\ N_\delta \end{bmatrix} \delta.
\end{aligned}
\tag{19}
$$

In term of control purpose, Eq. (19) is modified as

$$
\begin{aligned}
\dot v = \; & \frac{I_z - N_{\dot r}}{\nabla}((-Y_v - Y_{|v|v}|v| - Y_{|r|v}|r|)v + ((m - X_{\dot u})u_0 - Y_r - \\
& Y_{|v|r}|v| - Y_{|r|r}|r|)r + Y_\delta \delta) - \frac{m x_g - Y_{\dot r}}{\nabla}((-(m - X_{\dot u})u_0 - N_v - \\
& N_{|v|v}|v| - N_{|r|v}|r|)v + (-N_r - N_{|v|r}|v| - N_{|r|r}|r|)r + N_\delta \delta),
\end{aligned}
\tag{20}
$$

$$
\begin{aligned}
\dot r = \; & \frac{N_{\dot v} - m x_g}{\nabla}((-Y_v - Y_{|v|v}|v| - Y_{|r|v}|r|)v + ((m - X_{\dot u})u_0 - Y_r - \\
& Y_{|v|r}|v| - Y_{|r|r}|r|)r + Y_\delta \delta) + \frac{m - Y_{\dot v}}{\nabla}((-(m - X_{\dot u})u_0 - N_v - \\
& N_{|v|v}|v| - N_{|r|v}|r|)v + (-N_r - N_{|v|r}|v| - N_{|r|r}|r|)r + N_\delta \delta),
\end{aligned}
\tag{21}
$$

with $\nabla = (m - Y_{\dot v})(I_z - N_{\dot r}) - (m x_g - Y_{\dot r})(m x_g - N_{\dot v})$. As compared to the nonlinear steering model, the first order Nomoto model as the simplest set of describing yaw motion and the nonlinear extension of it are chosen. The formulations are respectively written as follows.

The first order Nomoto model is

$$T\dot r + r = K\delta, \tag{22}$$

the first order nonlinear Nomoto model is

$$T\dot r + n_3 r^3 + n_1 r = K\delta, \tag{23}$$

where T is the steering time constant, K is the rudder gain, n_3 is the coefficient of nonlinear item, and $n_1 = 1$ for the stable container ship [1].

Note that the 4 DOF dynamic model of the container ship is used to simulate maneuvers such as the straight line maneuver and the zigzag maneuver for testing the proposed model and parameter identification method. The roll effects considered in the 4 DOF model make the simulated maneuvers have similar features as the experimental data. But the simplified model without roll effects is to decrease the complexity of controller designs and eliminate challenges in parameter identification of the simplified model for ships even including the container ship.

3. Parameter identification using SVM optimized by ABC

3.1. SVM formulation

With several years application of SVM, it can also be designed to deal with sparse data in the condition of many variables and few data [21]. LS-SVM [22] is the one modified form of SVM, which has the ability to simultaneously minimize the estimation error in the training data (the empirical risk) and the model complexity (the structural risk) for both regression and classification. Consider a model in the primal weight space

$$y(x) = \omega^T \epsilon(x) + b(x \in R^n, y \in R), \tag{24}$$

where x is the input data, y is the output data, b is a bias term for the regression model, ω is a matrix of weights, and $\epsilon(\cdot) : R \to R^{n_h}$ is the mapping to a high-dimensional Hilbert space, the n_h can be infinite. The optimization problem in the primal weight space for a given training set $\{x_i, y_i\}_{i=1}^{N_s}$, with N_s as the number of samples becomes

$$\min_{w,b,e} J(\omega, e) = \frac{1}{2}\omega^T \omega + C\frac{1}{2}\sum_{i=1}^{N_s} e_i{}^2, \tag{25}$$

subject to

$$y_i = \omega^T \epsilon(x_i) + b + e_i, \tag{26}$$

where $e_i (i = 1, \ldots, N_s)$ are regression error, C is the regularization parameter, which should be always positive. In case of ω becoming the infinite dimension, the problem in the primal weight space cannot be solved. The Lagrangian is computed to derive the dual problem

$$J(\omega, b, e, \alpha) = J(\omega, e) - \sum_{i=1}^{N_s} \alpha_i (\omega^T \epsilon(x_i) + b + e_i - y_i), \tag{27}$$

where $\alpha_i (i = 1, \ldots, N_s)$ are the Lagrange multipliers. Now the derivatives with respect to ω, b, e_i, and α_i are computed and set to be zero, respectively

$$\begin{cases} \dfrac{\partial J(\omega, b, e, \alpha)}{\partial \omega} = 0 \to \omega = \displaystyle\sum_{i=1}^{N_s} \alpha_i \epsilon(x_i) \\ \dfrac{\partial J(\omega, b, e, \alpha)}{\partial b} = 0 \to \displaystyle\sum_{i=1}^{N_s} \alpha_i = 0 \\ \dfrac{\partial J(\omega, b, e, \alpha)}{\partial e_i} = 0 \to \alpha_i = Ce_i \\ \dfrac{\partial J(\omega, b, e, \alpha)}{\partial \alpha_i} = 0 \to \omega^T \epsilon(x_i) + b + e_i - y_i = 0 \end{cases} . \tag{28}$$

After straightforward computations, variables ω and e_i are eliminated from Eq. (28), and then the kernel trick is applied. The kernel trick can work in large dimensional feature spaces without explicit computations on them. Therefore, the problem formulation yields

$$y(x) = \sum_{i=1}^{N_s} \alpha_i K(x, x_i) + b, \tag{29}$$

where $K(x, x_i)$ represents the kernel function. Eq. (29) now can be applied to compute the regression model. For the problem of parametric identification, the linear kernel function is usually adopted, i.e., $K(x, x_i) = (x \cdot x_i)$, because the identification equations of simplified dynamic models are linear with respect to identification parameters. So the identified parameters ξ can be regressed by using the linear kernel based on LS-SVM, the regression model is

$$\xi = \sum_{i=1}^{N_s} \alpha_i x_i. \tag{30}$$

3.2. Regularization parameter selection based on ABC

After the linear kernel function in LS-SVM is decided, the performance of LS-SVM strongly depends on the regularization parameter. Thus, selection of regularization parameter for LS-SVM is one of the most important steps when using it as an identifier. According to [23], the grid search on the log-scale of the parameter in combination with cross-validation technique is commonly used to tune parameters in SVM. Even though this technique is simple, it is often time-consuming and at average accuracy [24]. From the extensive literature reviews, many different approaches have been proposed for tuning parameters in SVM. One widely-used technique is the swarm intelligence, for instance, the particle swarm optimization algorithm [15], the genetic algorithm [25], the firefly algorithm [26], and ABC [24], etc. Obviously, the design of the developed hybrid model is different regarding to the various problems needed to be solved in related domains. For the problem about parameter identification of the ship dynamic model, the hybrid approach of ABC with LS-SVM has not been applied. ABC proposed by Karaboga in 2005 is one of the most recent nature inspired algorithms based on foraging behaviors of bees, meanwhile, it has been proven being a robust and efficient algorithm for solving global optimization problems over continuous space [27]. So this paper uses ABC to optimize the regularization parameter in LS-SVM, and then applies LS-SVM with optimized parameter to estimate parameters of the simplified dynamic model of large container ships. The ABC consists of three groups of bees, i.e., employed bees, onlooker bees and scout bees, who play important roles in completing optimization procedure of ABC. The employed bees are responsible for exploring new food source positions in their neighbourhoods, evaluating the food quality (fitness value) of the new food sources, updating the current food sources, and sharing these information with onlooker bees waiting in hives. Onlooker bees choose a food source for exploration based on the information obtained from employed bees, and update food sources using the same way as employed bees. If an employed bee cannot improve its food source quality within a predefined number of iterations (*Limit*), it will become a scout bee. The scout bees will randomly find food sources within the search space. The details are explained as follows.

3.2.1. Key stages in ABC

Initialization The initial food sources randomly distributed within the search space are assigned to the employed bees. Every food source is an optimal solution, which includes the information

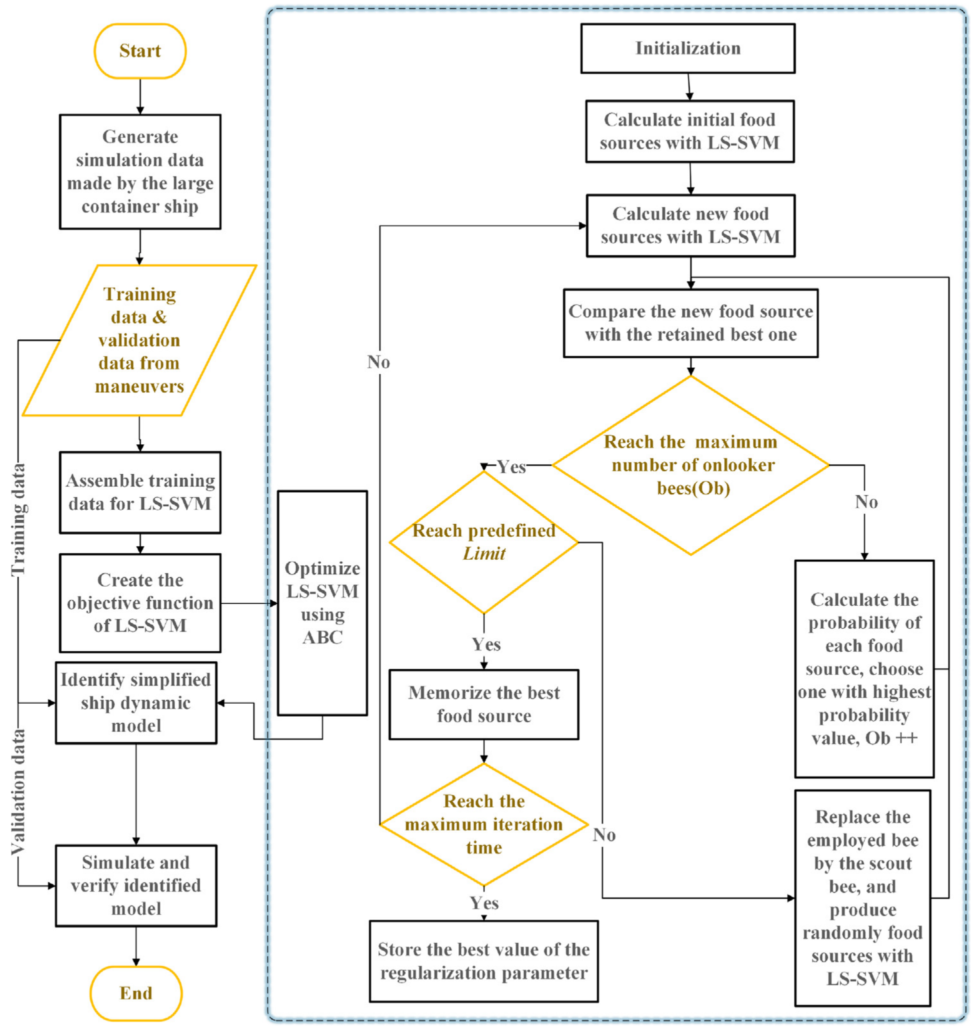

Fig. 2. Flowchart of ABC-LSSVM method.

of the food position and the food quality (fitness value). The food position is calculated by following equation

$$x_{ij} = x_j^{\min} + a(x_j^{\max} - x_j^{\min}),\ (i = 1, \ldots, S, j = 1, \ldots, D), \tag{31}$$

where $x_j^{\max}$ and $x_j^{\min}$ are the lower and upper bounds of the jth parameter respectively which decide the search space, a is random number in range of [0, 1], S is the number of food sources which is usually equal to the number of the employed bees donated as NP or the onlooker bees donated as NP, and D is the dimension conformed by the number of optimization parameter (here is 1). The fitness value $fitness_i$ is calculated as follows

$$fitness_i = \frac{1}{1 + Obj \cdot f \cdot_i}, \tag{32}$$

where $Obj. f._i$ is the objective function of the ith solution, which can be expressed as

$$Obj \cdot f \cdot_i = \frac{1}{N}\sum_{n=1}^{N}\left(y_{act}(n) - y_{pre}(n)\right)^2, \tag{33}$$

where y_{act} are actual outputs, y_{pre} are predicted outputs of identified models by LS-SVM, N is the number of samples.

The employed bees stage After initialization, employed bees start finding new food sources in their neighbourhoods according to the following equation

$$x_{ij}^{new} = x_{ij} + a(x_{ij} - x_{kj}),\ (i, k = 1, \ldots, S, j = 1, \ldots, D), \tag{34}$$

where x_{ij}^{new} is the jth dimension of the new food source, x_{kj} is the jth dimension of kth employed bee, a is a random number restricted in [−1, 1], jth and kth are randomly selected among initial solutions and are not equal to each other. The information of the ith new food source then are updated via Eqs. (32) and (33). The selection of new food source is decided by the greedy selection mechanism, i.e., if the fitness value of the new food source is better than the previous one, the new food source will replace the previous one, and *Limit* is set to zero, otherwise, the new food source will be ignored and *Limit* is added by one.

The onlooker bees stage The onlooker bees take food information from all employed bees. Every onlooker bee chooses a food source with a probability related to its fitness value. The probability is calculated as follows

$$p_i = \frac{fitness_i}{\sum_{i=1}^{S} fitness_i}. \tag{35}$$

Obviously, the higher fitness value the food source is, the better the food source is. In other words, the food source with high fitness value is more possible to be selected by onlooker bees. Then,

Table 3
The scheme of ship maneuvers.

Maneuver	Rudder angle (°)	Propeller shaft speed (rpm)	Purpose
Straight line	0	Vary in [120, 160]	Identify the surge model
Straight line	0	Vary in [100, 160]	Verify the identified surge model
20°/20° zigzag	±20	80	Identify the steering model
25°/25° zigzag	±25	80	Verify the identified steering model

Note that these maneuvers have the same initial conditions as follows: $U_0 = u_0 = 8$ m/s, $v_0 = 0$, $r_0 = 0$, $\delta_0 = 0$, $\psi_0 = 0$, $n_0 = 80$ rpm, the sample time is 900 s, and the interval is 0.5 s.

the procedure of updating food sources used by employed bees is also applied to onlooker bees. If the fitness value of the new food source calculated for onlooker bees is better than employed bees, the employed bee is replaced by the onlooker bee.

The scout bees stage If an employed bee cannot improve its food source quality within a predefined number (*Limit*), it will become a scout bee. The scout bees will randomly find food sources within the search space using Eq. (31).

3.2.2. Flow of ABC-LSSVM method

After obtaining the tuned regularization parameter of LS-SVM through ABC, LS-SVM is used to identify parameters of the simplified ship dynamic model. The cooperation of these procedures are called ABC-LSSVM method which is depicted in Fig. 2. The steps of this method are described as follows Step 1Simulate data by using a complex nonlinear model with predetermined parameter values of the large container ship. To turn LS-SVM by ABC for identifying the speed model, 1800 pairs of surge speed and corresponding actual propeller shaft speed extracted from the first straight line maneuver of the container ship as described in Table 3 are needed. Similarly, for identifying the steering model, same numbers of sway speed, yaw rate and related actual rudder angle obtained from the 20°/20° zigzag maneuver as presented in Table 3 are required. The extracted simulated data such as surge speed, sway speed and yaw rate are used as actual output to calculate the value of the objective function which is applicable to provide the food source the fitness value.Step 2Select the above extracted data to tune regularization parameter in LS-SVM based on ABC. This step is summarized as follows:Step 2.1Confirm the parameters of ABC, such as the number of food sources S or the number of employed bees or onlooker bees NP, the maximum iteration T, and the special number *Limit*, and finish the initialization (key steps in ABC).Step 2.2Search the new food sources by employed bees using Eq. (34), update the information of the new food sources, and select the new solution by the greedy selection mechanism.Step 2.3Onlooker bees get information from all employed bees and choose the food sources according to Eq. (35), and follow the same procedure as employed bees to update information of new food sources.Step 2.4Compare the new food source with the retained best one, judge whether the current number of onlooker bees equals to the total number or not. If so, judge whether the number of mining the same food source is larger than *Limit* or not, otherwise, increase the number of onlooker bees and return to step 2.3. If the number of mining the same food source reaches *Limit*, memorize the best food source, otherwise, produce new food source and return to step 2.3.Step 2.5Calculate current iteration number. If it reaches T, store the final result for regularization parameter, otherwise, return to step 2.2.Step 3Apply the training data and result of step 2.5 to LS-SVM in combination with the simplified ship dynamic model, then get the identified model.Step 4Combine the identified model and the series of actual propeller shaft speed and rudder angle respectively extracted from the rest two groups of maneuvers presented in Table 3 to predict and compare the outputs to verify the identified model and the optimized parameter for LS-SVM.

3.3. Construction of samples for identification

Inspired by [5] about linearizing the drag speed model, this paper obtains the perturbation dynamics in the initial condition of the steady surge motion corresponding to the state and input values $u = u_0$, $v = 0$, $r = 0$, $\delta = 0$, and $n = n_0$. According to Eq. (18), the perturbation dynamic model is expressed as

$$\Delta\dot{u} = \frac{X_u + 2X_{|u|u}|u_0|}{m - X_{\dot{u}}}\Delta u + \frac{X_{uuu}}{m - X_{\dot{u}}}\Delta u^3 + \frac{2T_{|n|n}|n_0|}{m - X_{\dot{u}}}\Delta n, \tag{36}$$

with $\Delta u = u - u_0$, $\Delta n = n - n_0$. For building identification constructions of speed and steering models, the forward-difference approximation of Eulers stepping method is used to discrete these models into

$$\begin{aligned}\Delta u(k+1) &= \Delta u(k) + \frac{h(X_u + 2X_{|u|u}|u_0|)}{m - X_{\dot{u}}}\Delta u(k) + \frac{hX_{uuu}}{m - X_{\dot{u}}}\Delta u^3(k) \\ &+ \frac{2hT_{|n|n}|n_0|}{m - X_{\dot{u}}}\Delta n(k),\end{aligned} \tag{37}$$

$$\begin{aligned}v(k+1) &= v(k) + \frac{h(I_z - N_{\dot{r}})}{\nabla}((-Y_v - Y_{|v|v}\left|v(k)\right| - Y_{|r|v}\left|r(k)\right|)v(k) + \\ &((m - X_{\dot{u}})u_0 - Y_r - Y_{|v|r}\left|v(k)\right| - Y_{|r|r}\left|r(k)\right|)r(k) + Y_\delta\delta(k)) \\ &- \frac{h(mx_g - Y_{\dot{r}})}{\nabla}((-(m - X_{\dot{u}})u_0 - N_v - N_{|v|v}\left|v(k)\right| + N_\delta\delta(k) - \\ &N_{|r|v}\left|r(k)\right|)v(k) - (N_r + N_{|v|r}\left|v(k)\right| + N_{|r|r}\left|r(k)\right|)r(k)),\end{aligned} \tag{38}$$

$$\begin{aligned}r(k+1) &= r(k) + \frac{h(N_{\dot{v}} - mx_g)}{\nabla}((-Y_v - Y_{|v|v}\left|v(k)\right| - Y_{|r|v}\left|r(k)\right|)v(k) + \\ &((m - X_{\dot{u}})u_0 - Y_r - Y_{|v|r}\left|v(k)\right| - Y_{|r|r}\left|r(k)\right|)r(k) + Y_\delta\delta(k)) \\ &+ \frac{h(m - Y_{\dot{v}})}{\nabla}((-(m - X_{\dot{u}})u_0 - N_v - N_{|v|v}\left|v(k)\right| + N_\delta\delta(k) - \\ &-N_{|r|v}\left|r(k)\right|)v(k) - (N_r + N_{|v|r}\left|v(k)\right| + N_{|r|r}\left|r(k)\right|)r(k)),\end{aligned} \tag{39}$$

where h is the time interval, $k+1$ and k are two successive data. According to the form of SVM, the input–output pairs are obtained through discretized equations. The inputs are expressed as

$$\begin{aligned}\mathbf{X} &= [\Delta u(k), \Delta u^3(k), \Delta n(k)]^T_{3\times 1}, \\ \mathbf{Y} &= [v(k), \left|v(k)\right| v(k), \left|r(k)\right| v(k), r(k), \left|v(k)\right| r(k), \left|r(k)\right| r(k), \delta(k)]^T_{7\times 1}, \\ \mathbf{Z} &= [v(k), \left|v(k)\right| v(k), \left|r(k)\right| v(k), r(k), \left|v(k)\right| r(k), \left|r(k)\right| r(k), \delta(k)]^T_{7\times 1}.\end{aligned}$$

Let

$$\begin{aligned}\mathbf{A} &= [a_1 \quad a_2 \quad a_3]_{1\times 3}, \\ \mathbf{B} &= [b_1 \quad b_2 \quad b_3 \quad b_4 \quad b_5 \quad b_6 \quad b_7]_{1\times 7}, \\ \mathbf{C} &= [c_1 \quad c_2 \quad c_3 \quad c_4 \quad c_5 \quad c_6 \quad c_7]_{1\times 7},\end{aligned}$$

with

$$
\begin{aligned}
a_1 &= 1+\frac{h(X_u+2X_{|u|u}\,|u_0|)}{m-X_{\dot u}},\\
a_2 &= \frac{hX_{uuu}}{m-X_{\dot u}},\\
a_3 &= \frac{2hT_{|n|n}\,|n_0|}{m-X_{\dot u}},\\
b_1 &= 1+\frac{(N_{\dot r}-I_z)Y_v h+((m-X_{\dot u})u_0+N_v)(mx_g-Y_{\dot r})h}{\nabla},\\
b_2 &= \frac{-(I_z-N_{\dot r})Y_{|v|v}h+(mx_g-Y_{\dot r})N_{|v|v}h}{\nabla},\\
b_3 &= \frac{-(I_z-N_{\dot r})Y_{|r|v}h+(mx_g-Y_{\dot r})N_{|r|v}h}{\nabla},\\
b_4 &= \frac{(I_z-N_{\dot r})((m-X_{\dot u})u_0-Y_r)h+(mx_g-Y_{\dot r})N_r h}{\nabla},\\
b_5 &= \frac{-(I_z-N_{\dot r})Y_{|v|r}h+(mx_g-Y_{\dot r})N_{|v|r}h}{\nabla},\\
b_6 &= \frac{-(I_z-N_{\dot r})Y_{|r|r}h+(mx_g-Y_{\dot r})N_{|r|r}h}{\nabla},\\
b_7 &= \frac{(I_z-N_{\dot r})Y_\delta h-(mx_g-Y_{\dot r})N_\delta h}{\nabla},\\
c_1 &= \frac{-(N_{\dot v}-mx_g)Y_v h-(m-Y_{\dot v})((m-X_{\dot u})u_0+N_v)h}{\nabla},\\
c_2 &= \frac{-(N_{\dot v}-mx_g)Y_{|v|v}h-(m-Y_{\dot v})N_{|v|v}h}{\nabla},\\
c_3 &= \frac{-(N_{\dot v}-mx_g)Y_{|r|v}h-(m-Y_{\dot v})N_{|r|v}h}{\nabla},\\
c_4 &= 1+\frac{(N_{\dot v}-mx_g)((m-X_{\dot u})u_0-Y_r)h-(m-Y_{\dot v})N_r h}{\nabla},\\
c_5 &= \frac{-(N_{\dot v}-mx_g)Y_{|v|r}h-(m-Y_{\dot v})N_{|v|r}h}{\nabla},\\
c_6 &= \frac{-(N_{\dot v}-mx_g)Y_{|r|r}h-(m-Y_{\dot v})N_{|r|r}h}{\nabla},\\
c_7 &= \frac{(N_{\dot v}-mx_g)Y_\delta h+(m-Y_{\dot v})N_\delta h}{\nabla},
\end{aligned}
$$

then the outputs are $u(k+1)=\mathbf{AX}$, $v(k+1)=\mathbf{BY}$, $r(k+1)=\mathbf{CZ}$.

4. Identification results

4.1. Data preprocessing

Under a benign environment without external disturbances and measurement noises, the numerical simulation data are the clean data with similar features as the experimental data. The selected model of the container ship has been well proven by [1,18]. The corresponding maneuvering simulation data are controllable and used as the alternative of real maneuver data. The numerical simulation is beyond many financial and technical possibilities to do the similar simulation as we did here for potential field tests. Good examples refer to [11,28,29].

For parameter identification, the data used for learning and validation are produced by Eqs. (3)–(10) with parameters extracted from the study in [18]. Four groups of maneuver including two straight lines with varying propeller shaft speed for estimating the speed model and 20°/20°, 25°/25° zigzag tests for the steering model are carried out, respectively. The details are introduced in Table 3. Fig. 3 presents the data produced for optimizing regularization parameter and identifying parameters of speed and steering models.

4.2. Identified models

Based on the flow of ABC-LSSVM method proposed in Section 3.2.2, the practical procedure for tuning the regularization parameter in LS-SVM by ABC can be concretely depicted as follows: (1) the properties of ABC are set as: $NP = 20,\quad S = 10,\quad D = 1,\quad x_j^{\min} = 10^{-2},\quad Limit = 20,\quad T = 30$; (2) the initial positions of food sources are calculated by Eq. (31); (3) employed bees start searching new food sources through Eq. (34). The selected data including 1800 samples extracted from the first straight line motion of the container ship and 1800 samples of 20°/20° zigzag maneuver are respectively applied to Eq. (33) to compute the fitness value via Eq. (32) for every food source; (4) the best food source is determined by the greedy selection mechanism and replaces the previously restored one. The value of the position of the best food source is the optimal regularization parameter; (5) onlooker bees take food information from employed bees. Eq. (35) is used to choose a food source for every onlooker bee. The food sources of onlooker bees are updated via Eqs. (32) and (33); (6) the employed bee will be replaced by the onlooker bee or the scout bee in two conditions, respectively: a. the updated fitness value of the food source of the onlooker bee is higher than the employed bee; b. the food fitness of the employed bee is not improved; (7) finally, the position of the food source with highest fitness value is defined as the optimal regularization parameter when the iteration number is 30.

The best regularization parameters for identifying speed and steering models are selected and recorded in Table 4. The ABC-LSSVM regression results are shown in Fig. 4, in which the approximations of LS-SVM agree well with the simulations, and the mean squared errors between prediction and simulation results (MSE) of u (8.3332×10^{-5}), MSE of v (5.7881×10^{-6}), and MSE of r (1.1455×10^{-5}) are small enough to be ignored. The optimized LS-SVM is subsequently used to identify the simplified ship dynamic model. The identification results, namely the parameters in **A**, **B**, and **C**, are given in Table 4.

4.3. Verification and comparison

4.3.1. Generalization verification

Generalization verification of identification results is an essential procedure for parameter identification. Hence, 25°/25° zigzag maneuver is predicted by using the identified models. The original simulated data of the 25°/25° zigzag maneuver are generated by the 4 DOF model of the container ship. As presented in Fig. 5, the prediction data are very similar to the original simulation in sway and yaw motion, which indicates that the identified steering model has satisfied agreement with the ones of the complex nonlinear large container ship. The predicted speed is a little higher than the simulated speed, but it can still illustrate that ABC-LSSVM performs good generalization because the small errors in surge speed predictions are not significant for practical aspects or to affect the applicability of the ABC-LSSVM method. It is worth to be noticed that the errors existing in surge speed predictions make few influences on the goal of this research which is to test and verify the applicability and effectiveness of the proposed ABC-LSSVM method to identify the simplified ship dynamic model. Furthermore, what causes these errors and how to improve the prediction accuracy will be the forthcoming studies.

For control purposes, the required model of the container ship dynamics yields as follows

$$
\begin{aligned}
\dot u &= -1.0059u-3.321\times10^{-5}u^3+0.1072\times10^{-4}\,|n|\,n,\\
&\quad\left(\frac{X_u+X_{|u|u}\,|u_0|}{m-X_{\dot u}}=-1.0059\,when\quad u_0=8\,\mathrm{m/s}\right),\\
\dot v &= 0.0857v-6.5552\,|v|\,v+28.4032\,|r|\,v+0.0134r+27.6766\,|v|\,r\\
&\quad+14.1552\,|r|\,r-0.0129\delta,\\
\dot r &= 1.9051v-3.1537\times10^{-4}\,|v|\,v+0.1203\,|r|\,v+2.0004r+0.3168\,|v|\,r\\
&\quad+16.5289\,|r|\,r+9.8642\times10^{-4}\delta.
\end{aligned}
\tag{40}
$$

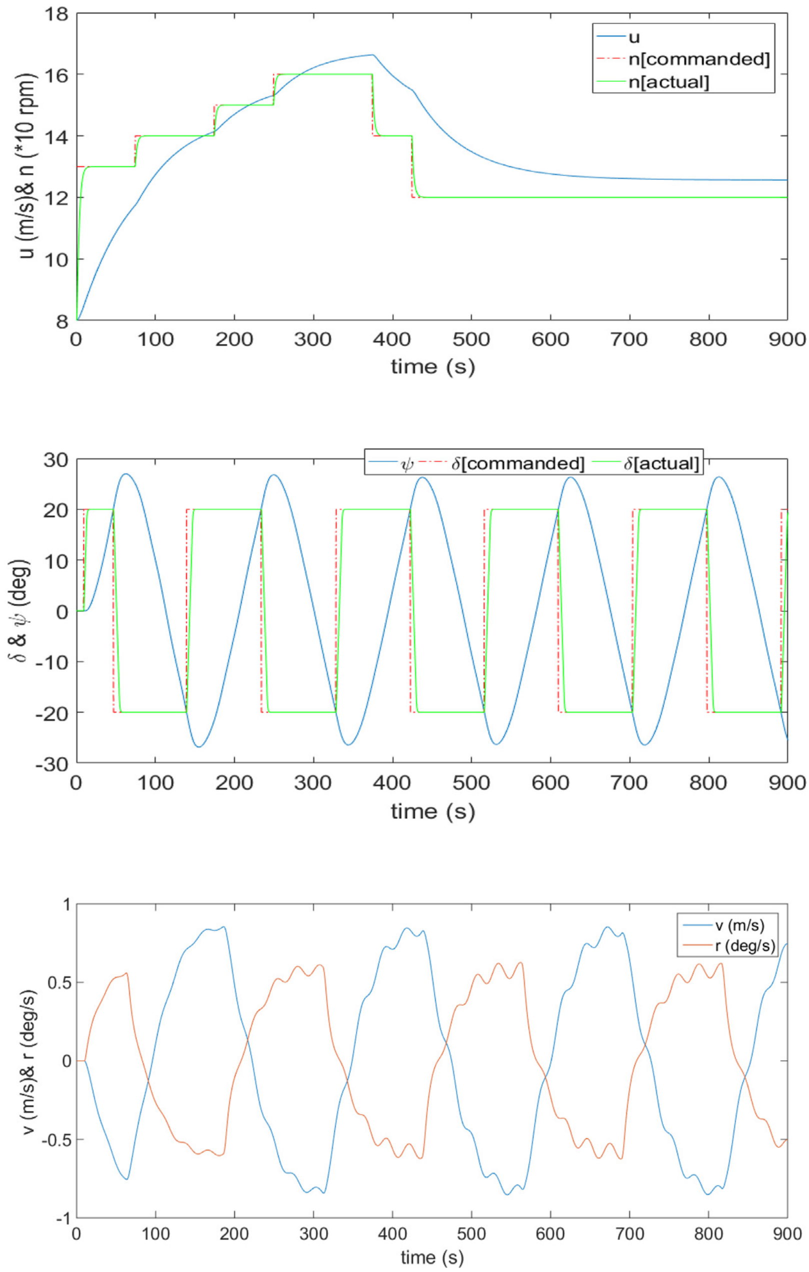

Fig. 3. Simulation data for optimization and identification of parameter: the upper sub-figure presents the surge speed of the first straight line maneuver as described in Table 3; the middle sub-figure donates the heading and rudder angles of the 20°/20° zigzag maneuver; the lower sub-figure is the sway speed and yaw rate of the 20°/20° zigzag maneuver.

Table 4
Identified parameters by CV-LSSVM, PSO-LSSVM, and ABC-LSSVM.

A(*)	CV	PSO	ABC	**B**	CV	PSO	ABC	**C**	CV	PSO	ABC
a_1	99420	99420	99410	b_1	0.9572	0.9571	0.9571	c_1	0.9524	0.9526	0.9525
a_2	−1.8595	−1.8807	−1.6605	b_2	−3.2528	−3.2776	−3.2776	c_2	−0.0002	−0.0002	−0.0002
a_3	86.154	86.153	85.794	b_3	14.0913	14.2017	14.2016	c_3	0.06	0.0603	0.0602
				b_4	0.007	0.0067	0.0067	c_4	−0.0002	−0.0002	−0.0002
				b_5	13.6556	13.8381	13.8383	c_5	0.1587	0.1581	0.1584
				b_6	6.7328	7.0606	7.0776	c_6	8.2971	8.2382	8.2645
				b_7	−0.0065	−0.0065	−0.0065	c_7	0.0005	0.0005	0.0005

Note:(CV) CV-LSSVM; (PSO) PSO-LSSVM; (ABC) ABC-LSSVM; (*) means ($\times 10^{-5}$).

4.3.2. Comparisons among different identification methods

In order to indicate the effectiveness of ABC-LSSVM, the comparisons of LS-SVM optimized by cross-validation technique (CV-LSSVM), and by PSO (PSO-LSSVM) have been carried out. The properties are set to the same values for both CV-LSSVM and PSO-LSSVM. For quantitatively analyzing and comparing the performance of these three parameter identification methods, three indexes such as the computational time, the best regularization

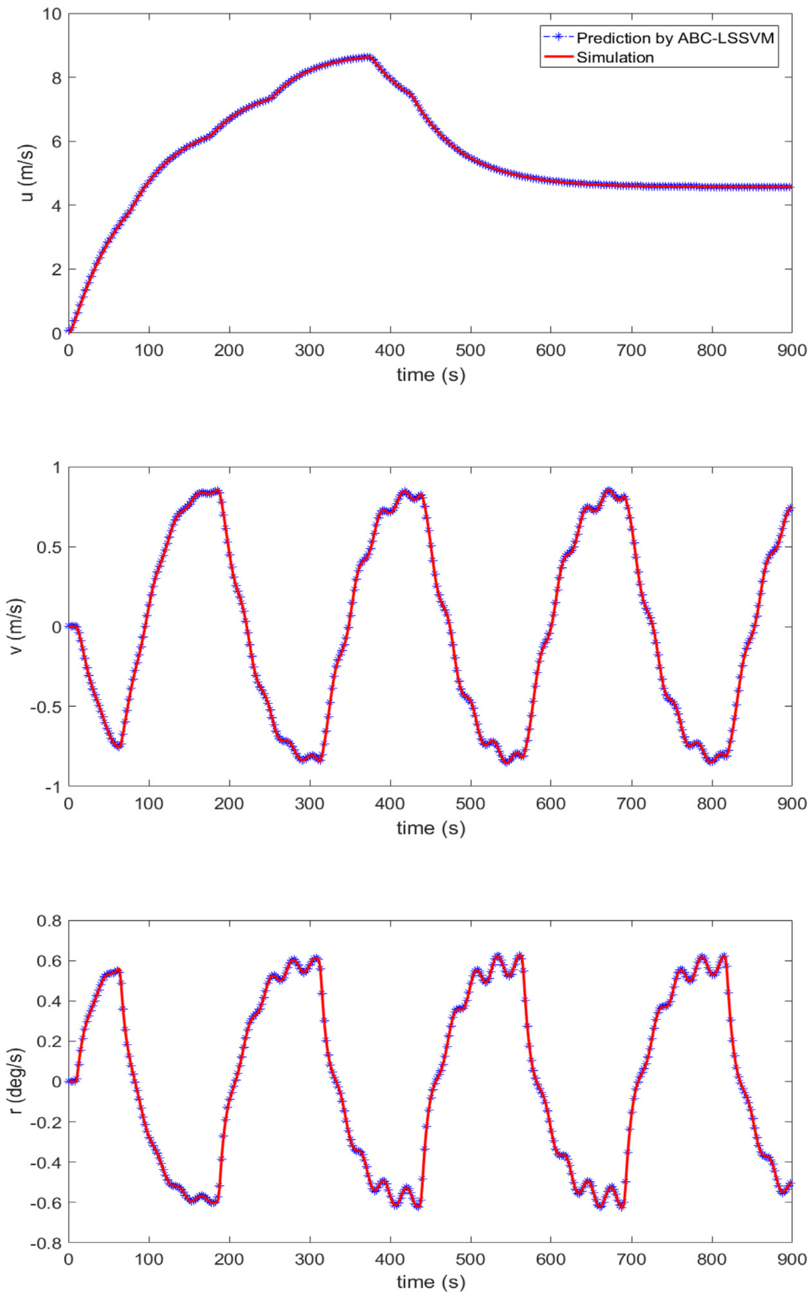

Fig. 4. ABC-LSSVM regression: the upper sub-figure is the surge speed of the first straight line maneuver; the middle sub-figure is the sway speed of the 20°/20° zigzag maneuver; the lower sub-figure is the yaw rate of the 20°/20° zigzag maneuver.

Table 5
Comparisons of the computational time, the best regularization parameter and MSE.

Method	Computation time (s)			Best regularization value ($\times 10^7$)			MSE ($\times 10^{-5}$)		
	SM	SS	SY	SM	SS	SY	SM (m^2/s^2)	SS (m^2/s^2)	SY ($^{\circ 2}/s^2$)
CV	0.3591	0.2603	0.2639	1.0196	97.12	494.92	5563	1.9669	0.28483
PSO	0.2867	0.2583	0.2531	1.2877	964.34	958.49	4734	1.9199	0.27934
ABC	0.2726	0.2460	0.2308	1.3175	600.00	578.61	4474	1.9050	0.12192

Note: (SM) surge model; (SS) Steering model (sway motion); (SY) Steering model (yaw motion); (CV) CV-LSSVM; (PSO) PSO-LSSVM; (ABC) ABC-LSSVM.

parameter and MSE are recorded in Table 5. The prediction results of 25°/25° zigzag maneuver are shown in Fig. 5. As seen, these three identification methods give a good prediction of 25°/25° zigzag maneuver. In other words, ABC-LSSVM, PSO-LSSVM and CV-LSSVM can identify the simplified dynamic models of ships and present a very similar performance. In some degree, the very slight differences existing in every index are not significant for practical aspect, but these differences make sense to conclude that the performance of ABC-LSSVM is slightly superior to the other two methods from the scientific research point of view.

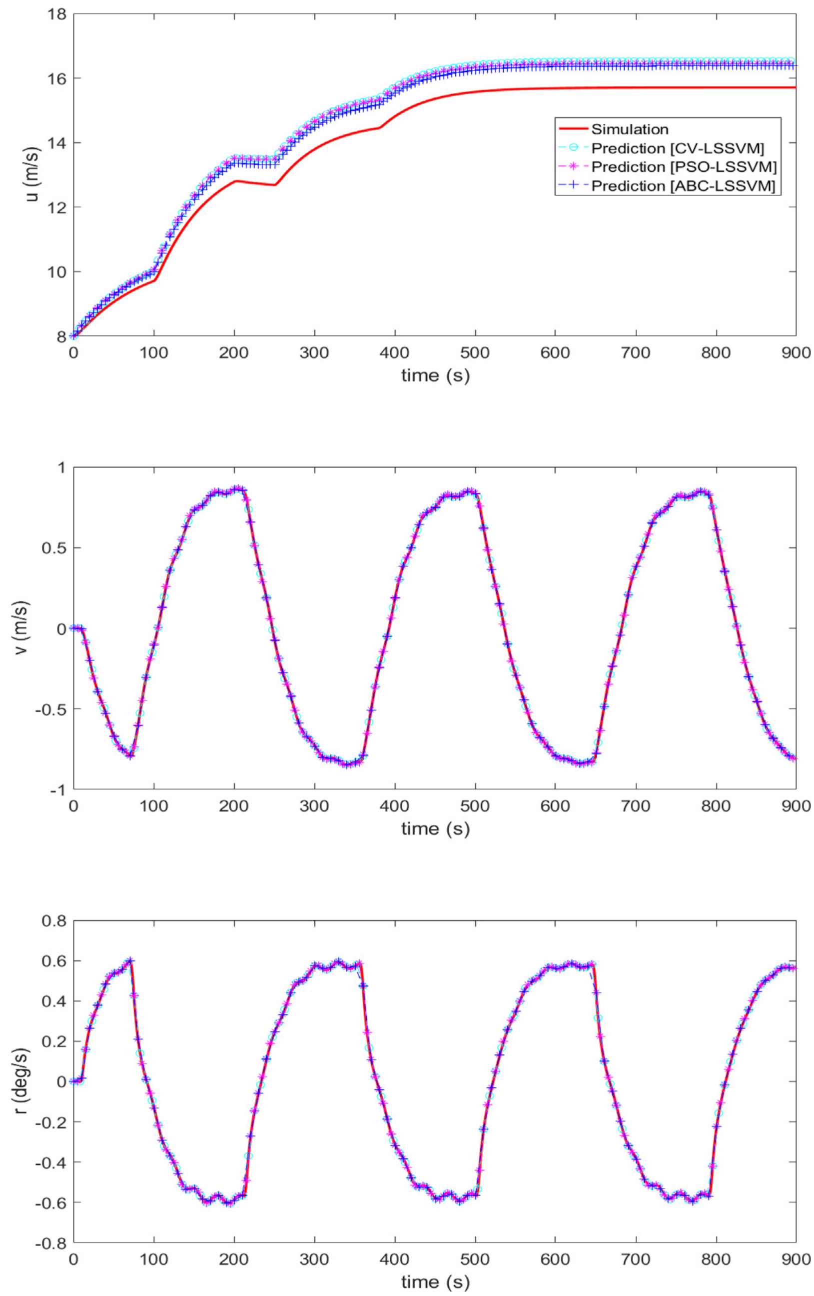

Fig. 5. Prediction of different identified ship dynamic models: the upper sub-figure is the surge speed of the second straight line maneuver as described in Table 3; the middle sub-figure is the sway speed of the 25°/25° zigzag maneuver; the lower sub-figure is the yaw rate of the 25°/25° zigzag maneuver.

From the numerical simulation study, the different characteristics of these optimization methods are observed and concluded. CV as trail and error method is a little time-consuming to find the suitable solution for current problem. The solution is not so optimal as the optimization results of PSO and ABC. PSO can find the global optimum for SVM, but sometimes it fails to provide globally optimal solutions instead of locally optimal ones. Comparatively, ABC shows relatively strong global optimization ability during the selection of regularization parameter of SVM procedure. As a consequence, CV could be an option for selecting parameters in SVM based on reliable experiences, and CV-LSSVM is suitable for offline parameter identification. ABC would be better than PSO to optimize SVM, and the combination of ABC and modified LS-SVM could be a potential application to online parameter identification in terms of computational time and finite samples.

4.3.3. *Comparisons among different steering models*

The data and ABC-LSSVM used for the nonlinear steering model are also utilized to identify and verify Nomoto models. The predictions of 25°/25° zigzag maneuver by these three steering models are shown in Fig. 6, and the identification results of the steering quality indices and the related MSE are given in Table 6. It can be observed that the performance of two Nomoto models is almost the same on account of the MSE. However, the nonlinear steering model shows better performance than these Nomoto models in terms of MSE. Therefore, for a container ship, the nonlinear steering model would be the best selection because it combines the coupling effects between sway and yaw motions, and can capture some nonlinear dynamics. If the robust controller is provided, the first order linear/nonlinear Nomoto model will be the good choice because of its simple construction.

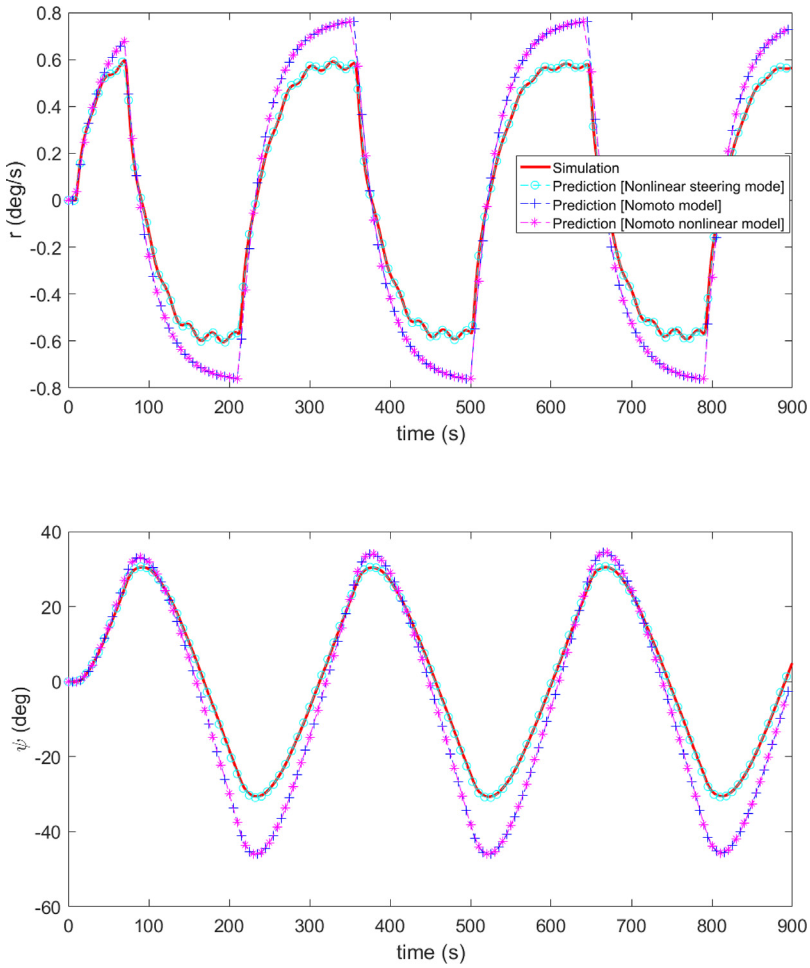

Fig. 6. Prediction of 25°/25° zigzag maneuver by different steering models.

Table 6
Identification results of Nomoto models.

Model	$K\,(1/s)$	$T\,(s)$	$n_3\ (\times 10^{-11})$	MSE [SY($^{\circ 2}/s^2$)]
NSM				1.219×10^{-4}
NM	0.031	30.2487		0.0168
NNM	0.031	30.2487	7.0853	0.0168

Note: (NM) the first order linear Nomoto model; (NNM) the first order nonlinear Nomoto model; (SY) Steering model (yaw motion); (NSM) the nonlinear steering model (yaw motion).

5. Conclusions

For the purpose of control designs for large ships, this paper introduced the concept of using simplified models to capture highly nonlinear dynamics of a large container ship. For the first time, ABC-LSSVM was used to identify the simplified dynamic models of large ships by using the simulated data made by the 4 DOF dynamic model of the container ship with known parameter values. As compared to the first order Nomoto models, the simplified nonlinear steering model can capture more complex dynamics of large ships because it considers the coupling effects between sway and yaw motions. The comparisons among CV-LSSVM, PSO-LSSVM and ABC-LSSVM indicate that the identified simplified ship dynamic models by these three methods show very good prediction results with small MSEs. ABC-LSSVM is relatively convenient and effective for parameter identification of ship dynamic models. Forthcoming work will focus on using real maneuvers' data extracted from experiments of large ships in combination with ABC-LSSVM to identify the simplified dynamic model. Then the robust controller will be designed to compensate for the prediction errors due to environmental influences, un-modeled coupling dynamics, etc.

Acknowledgements

The work described in this paper was supported by the Ministry of Science and Culture of Lower Saxony for funding the Graduate school of Safe Automation of Maritime Systems (SAMS).

References

[1] T.I. Fossen, Handbook of Marine Craft Hydrodynamics and Motion Control, John Wiley & Sons, 2011.
[2] S.-R. Oh, J. Sun, Z. Li, E.A. Celkis, D. Parsons, System identification of a model ship using a mechatronic system, IEEE/ASME Trans. Mechatron. 15 (2) (2010) 316–320.
[3] T.I. Fossen, Guidance and Control of Ocean Vehicles, John Wiley & Sons Inc., 1994.
[4] Z. Zwierzewicz, On the ship course-keeping control system design by using robust feedback linearization, Pol. Marit. Res. 20 (1) (2013) 70–76.

[5] C.R. Sonnenburg, C.A. Woolsey, Modeling, identification, and control of an unmanned surface vehicle, J. Field Robot. 30 (3) (2013) 371–398.
[6] R. Skjetne, O. Smogeli, T.I. Fossen, Modeling, identification, and adaptive maneuvering of cybership II: a complete design with experiments, Proc. IFAC Conf. on Control Applications in Marine Systems (2004) 203–208.
[7] F. Xu, T. Xiao, X. Xing, Z. Liu, Identification of Nomoto models with integral sample structure for identification, in: 2014 33rd Chinese Control Conference (CCC), IEEE, 2014, pp. 6721–6725.
[8] L. Ljung, Perspectives on system identification, Annu. Rev. Control 34 (1) (2010) 1–12.
[9] K.J. Åström, C. Källström, Identification of ship steering dynamics, Automatica 12 (1) (1976) 9–22.
[10] L.P. Perera, P. Oliveira, C.G. Soares, System identification of nonlinear vessel steering, J. Offshore Mech. Arct. Eng. 137 (3) (2015) 031302.
[11] G. Rajesh, S. Bhattacharyya, System identification for nonlinear maneuvering of large tankers using artificial neural network, Appl. Ocean Res. 30 (4) (2008) 256–263.
[12] S. Sutulo, C.G. Soares, An algorithm for offline identification of ship manoeuvring mathematical models from free-running tests, Ocean Eng. 79 (2014) 10–25.
[13] M. Zhu, A. Hahn, Y. Wen, A. Bolles, Parameter identification of ship maneuvering models using recursive least square method based on support vector machines, TransNav: Int. J. Mar. Navig. Saf. Sea Transp. 11 (1) (2017) 23–29.
[14] X.U. Feng, Z.J. Zou, J.C. Yin, C.A.O. Jian, Parametric identification and sensitivity analysis for autonomous underwater vehicles in diving plane, J. Hydrodyn. Ser. B 24 (5) (2012) 744–751.
[15] W. Luo, C.G. Soares, Z. Zou, Parameter identification of ship manoeuvring model based on particle swarm optimization and support vector machines, in: ASME 2013 32nd International Conference on Ocean Offshore and Arctic Engineering, American Society of Mechanical Engineers, 2013, V005T06A071.
[16] D. Karaboga, B. Akay, A comparative study of artificial bee colony algorithm, Appl. Math. Comput. 214 (1) (2009) 108–132.
[17] D. Karaboga, B. Gorkemli, C. Ozturk, N. Karaboga, A comprehensive survey: artificial bee colony (abc) algorithm and applications, Artif. Intell. Rev. 42 (1) (2014) 21–57.
[18] K.-H. Son, K. Nomoto, 5. On the coupled motion of steering and rolling of a high-speed container ship, Naval Archit. Ocean Eng. 20 (1982) 73–83.
[19] Z. Liu, Y. Zhang, X. Yu, C. Yuan, Unmanned surface vehicles: an overview of developments and challenges, Annu. Rev. Control 41 (2016) 71–93.
[20] R. Skjetne, Ø.N. Smogeli, T.I. Fossen, A nonlinear ship manoeuvering model: identification and adaptive control with experiments for a model ship, Model. Identif. Control 25 (1) (2004) 3.
[21] V. Vapnik, The Nature of Statistical Learning Theory, Springer Science & Business Media, 2013.
[22] J.A. Suykens, J. Vandewalle, Least squares support vector machine classifiers, Neural Process. Lett. 9 (3) (1999) 293–300.
[23] H. Frohlich, A. Zell, Efficient parameter selection for support vector machines in classification and regression via model-based global optimization, in: Proceedings 2005 IEEE International Joint Conference on Neural Networks, 2005, vol. 3, IEEE, 2005, pp. 1431–1436.
[24] M.H. Sulaiman, M.W. Mustafa, H. Shareef, S.N.A. Khalid, An application of artificial bee colony algorithm with least squares support vector machine for real and reactive power tracing in deregulated power system, Int. J. Electr. Power Energy Syst. 37 (1) (2012) 67–77.
[25] L. Dioşan, A. Rogozan, J.-P. Pecuchet, Improving classification performance of support vector machine by genetically optimising kernel shape and hyper-parameters, Appl. Intell. 36 (2) (2012) 280–294.
[26] T. Xiong, Y. Bao, Z. Hu, Multiple-output support vector regression with a firefly algorithm for interval-valued stock price index forecasting, Knowl. Based Syst. 55 (2014) 87–100.
[27] D. Karaboga, An idea based on honey bee swarm for numerical optimization, Tech. rep., Technical report-tr06, Erciyes University, Engineering Faculty, Computer Engineering Department, 2005.
[28] X.-R. Hou, Z.-J. Zou, Parameter identification of nonlinear roll motion equation for floating structures in irregular waves, Appl. Ocean Res. 55 (2016) 66–75.
[29] C. Jian, Z. Jiayuan, X. Feng, Y. Jianchuan, Z. Zaojian, Y. Hao, X. Tao, Y. Luchun, Parametric estimation of ship maneuvering motion with integral sample structure for identification, Appl. Ocean Res. 52 (2015) 212–221.